J|A|C|S COMMUNICATIONS

Published on Web 12/29/2009

Intermetallics as Novel Supports for Pt Monolayer O_2 Reduction Electrocatalysts: Potential for Significantly Improving Properties

Tanushree Ghosh,[†] Miomir B. Vukmirovic,[‡] Francis J. DiSalvo,[†] and Radoslav R. Adzic*[,‡]

Department of Chemistry and Chemical Biology, Cornell University, Ithaca, New York 14853, and Chemistry Department, Brookhaven National Laboratory, Upton, New York 11973

Received July 14, 2009; E-mail: adzic@bnl.gov

The insufficient catalytic activity and stability of Pt for the oxygen-reduction reaction (ORR) at fuel cell cathodes and its high content in catalysts remain major obstacles to the widespread commercialization of this technology. We describe one promising way of resolving these impediments with a class of electrocatalysts comprising a Pt monolayer deposited on intermetallic compound nanoparticles. The enhanced activity and stability of this class of electrocatalysts are derived from the combination of the unique properties of Pt monolayer catalysts and of the intermetallic compounds. Pt monolayers (Pt_{ML}) deposited on late-transition metals or their alloys exhibit high activity at ultralow Pt content.[1] Some intermetallic compound nanoparticles are stable and highly active catalysts for small organic molecule oxidation.[2,3] By combining these materials we obtain electrocatalysts that can overcome the above-named obstacles.

Here we report on the electrocatalytic properties of Pt_{ML} deposited on PtPb, PdPb, and PdFe intermetallic compound nanoparticles. The intermetallics with Pd afford an excellent support for a Pt_{ML}, while PdFe alloys have the advantage of being Pt-free, in addition to having high activity.[4,5]

Single-phase PtPb nanoparticles with a Pt:Pb molar ratio 1:1 and domain size 18 nm were synthesized by the coreduction of $Pt(acac)_2$ and Pb(2-ethylhexanoate) by sodium naphthalide in tetrahydrofuran (THF) at room temperature.[6] For PdFe, we synthesized primarily the alloy with the possible presence of an intermetallic phase. Further details on these syntheses appear in sections S1 and S2 in the SI. Figure S1-1 in SI shows the X-ray diffraction patterns for PtPb and PdPb, verifying the formation of intermetallic compounds in both.

Thin-film electrodes with nanoelectrocatalysts were fabricated by placing defined amounts of a nanoparticle suspension in H_2O (1 mg mL^{-1}) onto a flat glassy carbon electrode, 5 mm in diameter (Pine Instruments Co.). The initial voltammetry of the PdPb nanoparticles highlighted the dissolution of Pb, which subsided after several cycles (Figure S3-1a SI.). This finding indicated the presence of some Pb in the surface and subsurface layers. The Pt_{ML} was prepared by the galvanic replacement with Pt atoms of an underpotentially deposited (UPD) Cu monolayer on the catalyst electrode from a 50 mM H_2SO_4 + 50 mM $CuSO_4$ solution. All operations were done under an Ar atmosphere. The electrode covered with a Cu monolayer was rinsed and held in a 1.0 mM K_2PtCl_4 + 50 mM H_2SO_4 solution for about 3 min to ensure the complete replacement of Cu with Pt facilitated by a large difference in reversible potentials of Pt and Cu. A thin layer of Nafion was placed on the electrode to prevent its erosion during rotation.

Figure 1 shows the ORR polarization curves obtained with the Pt/PtPb, Pt/PdPb, and $Pt/PdFe_{550}$ electrocatalysts as a thin-film rotating disk electrode (RDE). The activities of these catalysts, expressed as half-wave potential, $E_{1/2}$, increase in the sequence: Pt/PdPb < $Pt/PdFe_{550}$ < Pt/PtPb. The very high activity of the Pt/PtPb catalyst is indicated by $E_{1/2}$ = 0.9 V, and a Pt monolayer mass activity of 0.97 A/mg at 0.9 V.

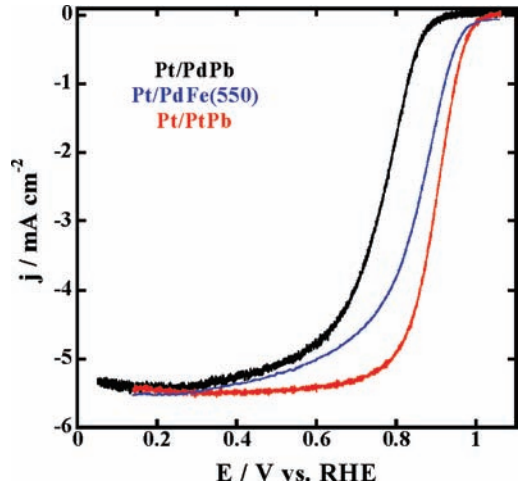

Figure 1. Polarization curves for the ORR on Pt/PtPb, Pt/PdPb, and $Pt/PdFe_{550}$ in 0.1 M $HClO_4$ solution at 1600 rpm; sweep rate 10 mV/s.

As expected, the substrate profoundly affects the activity of a Pt monolayer, which can be related to its d-band center position. The d-band center of metal monolayers, ε_d, is directly related to reactants' adsorption energies and activation barriers.[7] The position of the ε_d depends both on the strain (geometric effects), and on the electronic interaction between the Pt monolayer and the substrate (ligand effect). Since Pt replaces Pb and Fe from the top layer, and the resulting structures are overcompressed in Pt/PdFe and overexpanded in Pt/PdPb, the Pt/PtPd surface causing a slight compression is the most adequate substrate. These properties also affect the reactivity of Pt toward PtOH formation, which is the ORR inhibitor. On a Pt/PdPb catalyst PtOH occurs at more negative potentials than that observed for Pt nanoparticles (SI, Figure S3-1b). This indicates that this surface will not be a very active ORR catalyst, as is depicted in Figure 1. Thus, the Pd atoms in a surface layer are expanded because of the larger lattice and atomic size of Pb, thereby shifting positively d-band center, i.e., increasing the surface reactivity and favoring the easier formation of the oxide. Thus, the electronic property of the Pt monolayer, which depends on the cumulative contributions of lattice strain and ligand effect, is likely to account for the observed activities.[8]

Table 1 summarizes the results obtained with several catalysts. Among them, the most active in terms of half-wave potential is the Pt/PtPb electrocatalyst, in agreement with the above analysis. Due to the initial higher loading of the PtPb catalyst, the mass activities are low despite its high specific activity. To ameliorate this problem, we conducted experiments with lower initial loadings of PtPb and PdPb dispersed on a carbon support (Vulcan XC-72).

[†] Cornell University.
[‡] Brookhaven National Laboratory.

10.1021/ja905850c © 2010 American Chemical Society

Table 1. Comparison of Electrochemical Characteristics of the PtPb- and PdFe-Based Electrocatalysts

catalyst surface	$E_{1/2}$ (mV)	Pt (μg/cm^2)[a]	j_k (0.9 V) (mA/cm^2)[b]	Pt mass activity (0.9 V) (A/mg)	Pt_{ML} mass activity (A/mg)
PtPb	846	46	1.39	0.03	n.a.
Pt/PtPb	900	91	5.38	0.06	0.97
$Pt/PdFe_{550}$	848	4	2.17	0.54	0.54

[a] Calculated by adding the amount of Pt from the initial PtPb loading to the amount of Pt deposited by UPD wherever applicable. [b] Normalized to the electrode's geometric surface area (0.2 cm^2).

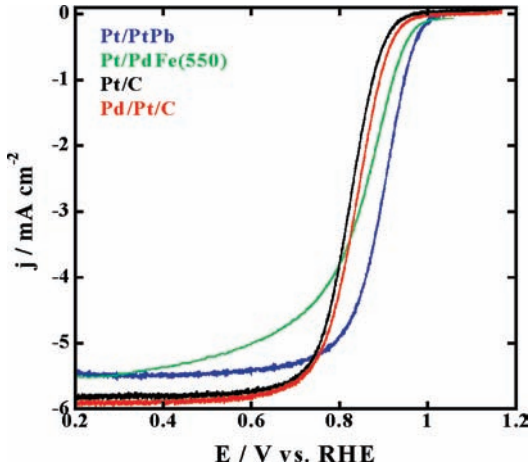

Figure 2. Comparison of the activities for the ORR of Pt/C, core−shell Pt_{ML}/Pd/C, and Pt/PtPb and Pt/PdFe in 0.1 M $HClO_4$; 1600 rpm; 10 mV/s.

The support ensured higher dispersion, even with a lower loading, and so the utilization of Pt becomes significantly higher while the electrode's conductivity is somewhat improved (Table S5-1, SI).

A comparison of the activities of standard Pt/C, core−shell Pt_{ML}/Pd/C, and the intermetallics-supported Pt/PtPb and Pt/PdFe electrocatalysts toward the ORR is given in Figure 2. The activity of a standard catalyst is inferior to those of Pt intermetallics. The activity of the catalysts in Figure 1 before and after the stability test is depicted in Figure 3. The Pt/PtPb catalysts produced currents at 0.9 V as high as 2.7 mA/cm^{-2} (geometric surface area). The stability of the catalysts was assessed by applying potential steps between 0.6 and 1.13 V at 10 s intervals. This is a more severe test than the DOE protocol with the 1.05 V positive potential limit. The unsupported catalysts showed no diminution in activity after 6000 cycles. However, a loss of activity was observed in the corresponding supported catalyst, suggesting that carbon corrosion or another problem related to the support was responsible for this effect. After 16,000 cycles, the unsupported catalysts showed a loss of activity, but it was recovered in its entirety by several potential cycles in a fresh electrolyte solution. Hence, contamination of the electrode surface by solution-phase species apparently accounted for the depletion of activity. Figure S4-1, SI, gives the polarization curves for the Pt/PtPb catalysts, illustrating these findings.

The PdFe samples investigated showed interesting morphologies and excellent activity, and the possible presence of additional functionalities warrant further studies (Figure S2-2, SI).

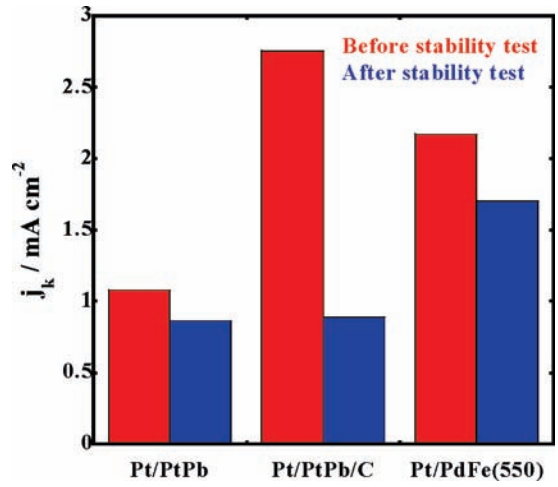

Figure 3. Bar plot of the kinetic current density at 0.9 V for the electrocatalysts in Figure 1 both before and after stability tests of 16,000 cycles (see text). The data for Pt/PtPb, Table 1 (lower initial PtPb loading).

In conclusion, we demonstrated the formation of a new class of core−shell electrocatalysts for the ORR, consisting of a Pt monolayer shell and ordered intermetallic compound cores. Thus, we coupled highly stable, inexpensive intermetallics with a Pt monolayer to produce electrocatalysts with high activity, low metal content, and very high stability. Our data indicate strategies suitable for selecting the types of intermetallic compounds as the support for a Pt monolayer. We consider that this fabrication method holds excellent potential for creating efficient fuel cell electrocatalysts.

Acknowledgment. This work has been supported by the U.S. Department of Energy, Divisions of Chemical and Material Sciences, under the Contract No. DE-AC02-98CH10886.

Supporting Information Available: Additional information on synthesis and characterization data for PdFe, PdPb, and PdPb systems. This material is available free of charge via the Internet at http://pubs.acs.org.

References

(1) Adzic, R. R.; Zhang, J.; Sasaki, K.; Vukmirovic, M. B.; Shao, M.; Wang, J. X.; Nilekar, A. U.; Mavrikakis, M.; Valerio, J. A.; Uribe, F. *Top. Catal.* **2007**, *46* (3−4), 249–262.
(2) Roychowdhury, C.; Matsumoto, F.; Zeldovich, V. B.; Warren, S. C.; Mutolo, P. F.; Ballesteros, M.; Wiesner, U.; Abruna, H. D.; DiSalvo, F. J. *Chem. Mater.* **2006**, *18* (14), 3365–3372.
(3) Alden, L. R.; Roychowdhury, C.; Matsumoto, F.; Han, D. K.; Zeldovich, V. B.; Abruna, H. D.; DiSalvo, F. J. *Langmuir* **2006**, *22* (25), 10465–10471.
(4) Shao, M. H.; Sasaki, K.; Liu, P.; Adzic, R. R. *Z. Phys. Chem.-Int. J. Res. Phys. Chem. Chem. Phys.* **2007**, *221*, 1175–1190.
(5) Shao, M. H.; Sasaki, K.; Adzic, R. R. *J. Am. Chem. Soc.* **2006**, *128* (11), 3526–3527.
(6) Ghosh, T.; Matsumoto, F.; McInnis, J.; Weiss, M.; Abruna, H. D.; DiSalvo, F. *J. Nanopart. Res.* **2009**, *11* (4), 965–980.
(7) Pallassana, V.; Neurock, M.; Hansen, L. B.; Hammer, B.; Norskov, J. K. *Phys. Rev. B* **1999**, *60* (8), 6146–6154.
(8) Greeley, J.; Mavrikakis, M. *Nat. Mater.* **2004**, *3* (11), 810–815.

JA905850C